Det Kgl. Danske Videnskabernes Selskab.
Mathematisk-fysiske Meddelelser. **XVIII**, 4.

CLOUD CHAMBER STUDIES OF FISSION FRAGMENT TRACKS

BY

J. K. BØGGILD, K. J. BROSTRØM

AND

T. LAURITSEN

KØBENHAVN
EJNAR MUNKSGAARD
1940

CONTENTS

Printed in Denmark.
Bianco Lunos Bogtrykkeri A/S.

1. Introduction.

Shortly after the discovery of the fission phenomenon, cloud chamber tracks of uranium fission fragments were published by JOLIOT (1), by CORSON and THORNTON (2) and by PERFILOV (3). Such tracks exhibit a very intense ionization along the paths of the fragments, as well as rather frequent branches due to close collisions with the nuclei of the atoms composing the gas in the chamber. These and other peculiar features of the tracks were clearly brought out in the course of a more complete study of the phenomenon at this Institute, of which a brief report (4) has already been published. In particular, it was shown that it is possible to obtain rough quantitative information about the penetration of such heavy particles through matter by a study of the branching of the tracks. Thus, measurements of branches in argon gas at various parts of the range showed that the velocity-range curve exhibits marked differences from that known for lighter particles, being characterized by an almost linear slope at the beginning of the range, flattening off appreciably toward the end of the range, and finally falling very sharply at the extreme end. Another interesting difference from the behaviour of light particles was illustrated in these pictures by the conspicuous tendency to gradual fortuitous bending of the fragment tracks, due to nuclear collisions not sufficiently close to give rise to observable branches.

In a note accompanying this preliminary report, Professor Bohr (5) pointed out that these effects could be understood as direct consequences of the high nuclear charge and large mass of the fragments. The high charge implies not only that electron capture into bound states with high energies will have a strong influence on the stopping phenomenon, but also that stopping by means of nuclear collisions will be important at relatively high velocities. While for the first part of the range the stopping due to electronic interactions is predominant, the effect of nuclear collisions becomes gradually more important near the end of the range and will not only give rise to the observed curvatures of the path but will even be mainly responsible for the stopping effect. The range-velocity curve will thus consist of two essentially different parts according to the relative importance of nuclear and electronic interactions. In the almost linear course of the curve for high velocities, we see the effect of the decrease of the total effective charge of the fragments, while in the steep decrease at the end of the range we have practically only to do with direct nuclear collisions. In the region between, where the velocity corresponds approximately to that of the most loosely bound electrons in the neutral atom, the particles lose momentum at a much slower rate than at any other part of the range, giving rise to an almost flat plateau in the curve.

In the first report, no attempt was made to distinguish between the tracks of fission fragments of different mass and charge. More recently, however, measurements of tracks from thin uranium targets have indicated the presence of two ranges which can be ascribed to the two main groups of fission fragments disclosed by direct measurements of

the ionization produced by individual fragments as well as by chemical analysis of the fission products (6 and 7). Furthermore, it was shown in this connection that a statistical analysis of the distribution of branches at different parts of the range of a large number of tracks definitely shows the presence of two distinct groups of tracks differing in their average number of branches. This analysis permitted moreover the construction of individual range-velocity curves for the two fragment types. The broad outlines of this work have been the subject of a recent note by Professor Bohr and the authors (8) and will be more fully discussed in the present paper which gives a complete account of the experimental work. The results of the experiments will be interpreted in close connection with the detailed theoretical treatment of the problem published separately by Professor Bohr (9).

2. Experimental Arrangement.

The tracks which were studied originated from fission of uranium produced by bombardment with slow neutrons. The uranium was mounted directly inside a 25 cm cloud chamber in such a way that the particles coming from the uranium layer suffered no other stopping than that due to the layer itself. In some experiments, a copper strip with a thick coating of uranium oxide was placed near the wall of the chamber; in others, a thin aluminum or mica foil with an evaporated deposit of uranium metal was suspended across the middle of the chamber to permit study of both fragments from a given fission process simultaneously. As a neutron source, beryllium bombarded with high energy deuterons was used. The deuteron beam was produced by the high tension installation recently completed at this Insti-

tute (10) and, in most of the experiments, a beam of about 100 microamperes at 800 kilovolts was focussed on a beryllium target inside the acceleration tube. The target tube and the cloud chamber, which were separated by about 10 cm, were surrounded as completely as practicable with paraffin to a thickness of 10 cm. A block of lead about 5 cm thick was introduced between the chamber and the target to absorb the gamma radiation from the target. Fig. 1 is a drawing of the complete arrangement, showing the location of the neutron source and cloud chamber and indicating the two alternative positions of the uranium.

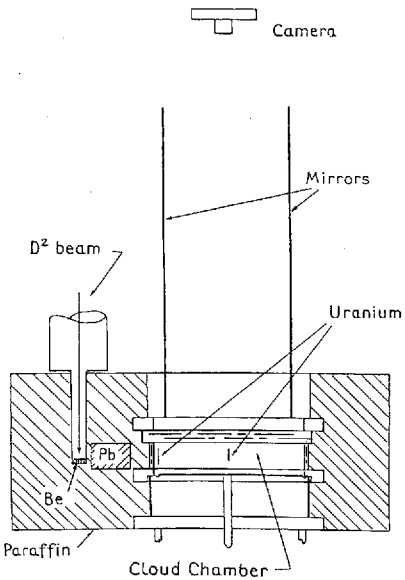

Fig. 1. Diagram of experimental arrangement showing neutron source, cloud chamber and system for stereoscopic photography of tracks.

In order to make investigation of the finest details of the tracks possible, the chamber was operated at reduced pressure, sometimes with hydrogen gas and sometimes with argon gas. In most cases, the vapor was furnished by a mixture of half ethyl alcohol and half water, although some pictures were taken with *n*-propyl alcohol mixture and some with water vapor only. Since the interaction of the fast neutrons coming directly from the beryllium target with the hydrogen atoms present in the gas produced an intense ionization due to proton recoils, it was necessary to take special precautions to insure an adequate sweep field to

clear the chamber of ions formed before the expansion. For this purpose, a voltage of 600 to 1000 volts was used, and the glass top of the chamber was covered with a layer of gelatine with fine metal wires to provide a conducting surface. The chamber was arranged to give a particularly rapid expansion which seemed to make the tracks stand out more sharply and which had the effect of keeping the background more clean.

Stereoscopic photographs were taken with a Leica camera and a double mirror system giving a direct image and two

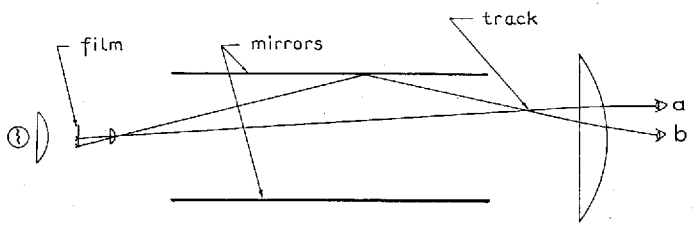

Fig. 2. Reprojection system for measurement of films.

half mirror images. Measurements on the films were carried out by means of the arrangement of Fig. 2, using the same mirrors and the same objective as in the original photography. The mirrors and the objective are held in a frame which can be removed from the cloud chamber to a position convenient for measurements, where the camera is screwed off its objective and replaced by a suitable projector. With this arrangement, a natural size image of the track in space is produced at a position corresponding to that of the cloud chamber and can be observed on a screen held in the correct plane. In order to see the track in space, one has simply to place one eye at "b" (in the figure) and the other at "a", so that the one eye sees the track as the camera saw it directly while the other sees it from a position corresponding

to the camera's mirror image. To collect light from the whole field, a large field lense is introduced, focussing the camera objective and its mirror image on the corresponding eyes. Actually, because of the two mirrors, three images are formed, from which the observer choses the two appropriate to the half of the chamber in which he is interested. It is then quite easy to introduce a scale or protractor and make the desired measurements on the natural size track. While some magnification is introduced by the field lense, this magnification is the same for both scale and track and hence does not enter the computations.

In all, some 8000 photographs have been taken; of these, 7000 with thick uranium layers have yielded 400 fragment tracks usable for branch studies, and about 1000 photographs with the thin foil arrangement have yielded 30 tracks suitable for range measurements.

3. General Features of Tracks.

Certain features of the fission fragment tracks are quite typical and make possible their immediate distinction from the alpha particle and proton tracks present as background in the cloud chamber. The most conspicuous of these characteristics is the intense ionization which is under certain conditions so striking that the tracks are instantly recognized visually at the time of their appearance in the chamber, even though there may at the same time be several alpha particle tracks and hundreds of proton recoils present. Any attempt at an absolute estimate of the ionization would be of very doubtful value, however, as the variations under different operating conditions are quite considerable, depending, for example, on the amount of vapor which has

been condensed out by the background radiations before the track appears. In fact, it occurs quite frequently that a fragment track shows a discontinuity caused by the reduction of the supersaturation by an earlier proton or alpha particle track along a line crossing the fragment's path. (See Plate IIa for example).

Another feature of the fragment tracks so common as to be distinguishing is the ejection of side branches by collisions with the atoms of the gas. Particularly in argon gas, practically every track has several conspicuous branches along its length; and that even the main body of the track contains a large number of short branches is shown by the pictures at low pressure in hydrogen. Here, because of the low stopping power, the branches project out of the general ionization region and give the track a hairy appearance similar to the effect of delta rays on alpha particle tracks, but with the difference that these side branches are straight and closely ionized, indicating that they are indeed proton tracks (see Plate IIb). The end of the range is uniformly characterized by a tuft consisting of several short branches. In all but a very few cases, it could be shown that the absence of such a tuft was due to the track's going out of the light region, or to "cutting" by an old track.

Not infrequently, especially in heavy gases, close collisions occur in which the projected particle gets a velocity greater than that of the fragment itself, resulting in a branch considerably longer than the residual range of the main track (see Plates IIIa, IIIb, IVa and IVb). Particularly when such branches appear very near the end of the range, it might be difficult to be certain which of the tracks belonged to the heavy particle, except for the characteristic tuft. In cases of close encounter at larger distances from the end

of the range, the ionizing power is seen to be abruptly decreased by the sudden fall in velocity, showing that a region of considerable length exists where the rate of energy loss is at a minimum, the rise at the end of the range being evident in the tuft formation. This conclusion is in agreement with the fact that long tracks seem more intense at the beginning of the range, but because of the possibility of variations in the sensitivity of the different regions of the cloud chamber, this observation is not at all so certain as the evidence of the sudden change in ionization accompanying violent collisions.

In general, the branches have considerable ionizing power as compared with the tracks of protons and alpha particles in the background, but occasionally, especially when a large proportion of the gas in the chamber is hydrogen, very fine branches appear which are so weak as almost to escape detection. It seems most probable that such branches are the result of collisions with hydrogen nuclei, which would not be expected to ionize as intensely as the heavier nuclei. Because these fine branches occur only in the best pictures, it is believed that hydrogen branches are not photographed except under special operating conditions, although they would otherwise be expected to be rather frequent in occurrence. It is quite possible that the sensitive time of the cloud chamber is considerably longer for the heavily ionizing particles than for such fine tracks. In connection with the pictures in argon, it has been noticed that the branches have often themselves branches (see Plates IIIb, IVa, and IVb) with, in rare instances, even tertiary branching, indicating that high speed argon nuclei have also a large probability for nuclear collisions, as would of course be expected from their high charge.

In marked contrast to the tracks of lighter particles, both the fission fragment tracks and their argon branches show a very conspicuous gradual bending due to collisions so small as not to be individually distinguishable in the photographs (see Plates IIa, IIIa and IVa). That this curvature is real and not a result of distortion in the cloud chamber is clear from the fact that the alpha particle and proton tracks in the background are quite straight, and that the curvature occurs practically only in the last part of the range, while the tracks are almost straight at the beginning. Also, the bending is very much less in the pictures in hydrogen gas than in those with argon. Because of this bending of the fission fragment tracks, measurements of the angles of deflection in collisions giving rise to visible branches are very difficult, particularly for branches occurring near the end of the range. Determinations of the mass ratios of the colliding nuclei from such measurements are therefore liable to considerable uncertainty, and it would, for example, not seem possible to distinguish between fragments of different masses by such measurements.

4. Paired Fragment Tracks.

In an attempt to determine the total ranges of the fission fragments, a number of pictures were taken in argon with thin evaporated layers of uranium (0.2 to 0.8 mg/cm²) on 0.3 mg/cm² aluminium foils or on 1.2 mg/cm² mica foils suspended across the middle of the cloud chamber. Typical examples of pairs of tracks obtained in this way are shown in Plates Va and Vb. Because of the extreme thinness of the layer and the increased distance from the neutron source, the yield of usable double tracks was very small and the

data obtained are not sufficient to permit more than rough estimates for the range. In the table are given the values obtained from 8 pairs of fragment tracks and 14 half-pairs in which one member did not end in the lighted part of the chamber; the visible lengths of such members are enclosed in parentheses.

In the absence of information on the relative stopping powers for fission fragments of the various substances present in the gas and vapor of the chamber, the lengths

Table of ranges of tracks from thin layers.

No.	Length in chamber A.	Length in chamber B.	Stopping power rel. norm. air	Reduced length short	Reduced length long	Reduced length sum
1.	45 mm	67 mm + 0.3 mg/cm² Al.....	0.37	16.5 mm	26 mm	42.5 mm
2.	76	59 „ „ „	0.33	22	25	47
3.	49	63 „ „ „	0.37	18	25	43
4.	68	52 „ „ „	0.37	21	25	46
5.	67	(>32) „ „ „	0.36	(>13)	24	—
6.	(>56)	49 „ „ „	0.33	18	(>19)	—
7.	(>50)	50 „ „ „	0.33	18	(>16.5)	—
8.	(>27)	45 „ „ „	0.35	17.5	(> 9.5)	—
9.	58	61 mm + 1.3 mg/cm² mica ..	0.315	18	28	46
10.	80	35 + 1.2 „ „ ..	„	19	25	44
11.	88	33 + 1.3 „ „ ..	„	19	27.5	46.5
12.	69	38 + 1.3 „ „ ..	„	22	22	44
13.	51	(>27) + 1.6 „ „ ..	„	16	(>22)	—
14.	63	— — „ „ ..	„	19.5	—	—
15.	75	(>26) + 1.3 „ „ ..	„	(>21)	24	—
16.	90	(>24) + 1.3 „ „ ..	„	(>22)	28.5	—
17.	87	— — „ „ ..	„	—	27.0	—
18.	—	35 + 1.2 „ „ ..	„	19	—	—
19.	(>36)	43 + 1.6 „ „ ..	„	(>11)	24.5	—
20.	62	— — „ „ ..	„	19.5	—	—
21.	—	43 + 1.6 „ „ ..	„	—	24.5	—
22.	54	— — „ „ ..	„	17.5	—	—
			Averages ...	19 ± 2	25 ± 2	45 ± 3

of the tracks have been reduced to air equivalent values by using the coefficients appropriate to alpha particles of similar velocities. Inasmuch as the pressures are nearly the same for all the tracks, this procedure will introduce an uncertainty only in the absolute values.

In the experiments using mica foils, the stopping power of the gas was directly measured by means of a beam of polonium α-particles admitted through a window in the side of the cloud chamber. In these experiments, the thickness of the foil necessitated a correction for the oblique passage of the particle inserted in the table.

The data seem to indicate the presence of two ranges, at 19 and 25 mm normal air, although the variation of individual values is rather large. The presence of these two ranges is consistent with the existence of two main groups of fission products, known from other lines of investigation where it has been shown that the most probable values of the masses of the two fragments resulting from the fission of uranium are 93 and 140 mass units. Taking their energies as 97 and 65 Mev. we get velocities of 14×10^8 and 9.3×10^8 cm/sec., respectively. Since from the general characteristics of the velocity-range curve, it appears quite certain that the particle with the smaller mass and the higher velocity will have the longer range (cf. ref. 8), we shall in the following assign the values in this order as one point on the range velocity curve for each particle.

5. Statistics of Branch Distribution.

In addition to the small amount of material obtained from thin uranium layers, a large number of tracks were photographed using thick targets and low gas pressures in

the cloud chamber to permit a closer investigation of the branching phenomenon. Especially has the study of branches on about 300 tracks in argon gas yielded many interesting results. The counting of the number of branches in various intervals of the range has, in fact, not only given information about the velocity-range relation, as discussed in the next section, but a statistical analysis of the distribution of the number of branches per track at various parts of the range has disclosed the presence of two groups of tracks differing markedly in their average number of branches.

In view of the fact that the average number of clearly visible branches per fragment track in argon under the present conditions is only about four, and since the numbers per track are distributed in an entirely fortuitous manner, it is impossible to distinguish the groups on the basis of differences between individual tracks. However, as indicated in the previous note (8), the presence of the groups can be recognized from the manner in which the number of branches per track is distributed. In fact, if the probability of branching in the region of the range considered were the same for all tracks, the probability for the occurrence of just n branches on a given track should be given by the formula

$$P(n) = \frac{\omega^n}{n!} e^{-\omega}$$

where ω is the mean branch number. If, on the other hand, we have to do with two groups of tracks occurring with equal frequency, the distribution is given by the expression

$$P(n) = \frac{1}{2}\frac{\omega_1^n}{n!} e^{-\omega_1} + \frac{1}{2}\frac{\omega_2^n}{n!} e^{-\omega_2}$$

where ω_1 and ω_2 are the mean values of branch numbers within each group, and $\frac{1}{2}(\omega_1 + \omega_2)$ is the average branch number for the whole ensemble. It is to be observed that the validity of this law of distribution is independent of any particular choice of counting method or other limitation, provided only that all tracks are treated alike.

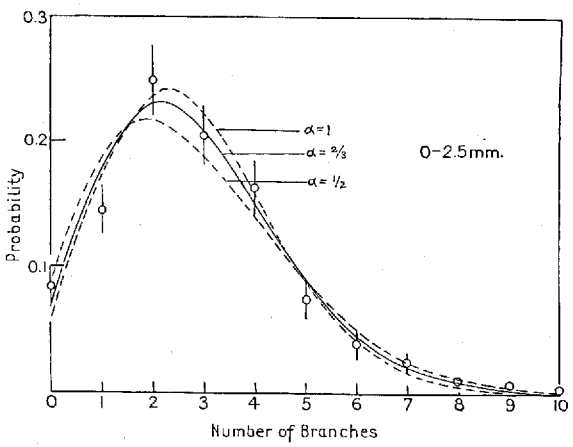

Fig. 3. Distribution of number of branches per track in region 0 to 2.5 mm from end of range.

The tracks used in the experimental study were taken in argon gas at about 7.5 cm pressure, with alcohol and water as the vapor source. Branches between two and ten millimeters length in the chamber were counted in the intervals from 0 to 20 mm and from 20 to 80 mm from the end of the range, corresponding to about 0 to 2.5 mm and 2.5 to 10 mm normal air. The fractions of the total number of tracks with given branch numbers are plotted as open circles in Figs. 3 and 4, of which the first refers to the range interval 0—2.5 mm and the second to the interval 2.5—10 mm. The material for Fig. 3 is derived from a count of

about 900 branches and that for Fig. 4 from about 350 branches; the probable errors of the probabilities $P(n)$ deduced from the counts are indicated by the vertical lines through the points. For comparison, curves representing the distributions to be expected for various values of the ratio $\alpha = \frac{\omega_1}{\omega_2}$ are plotted. While for Fig. 3, the deviation from the

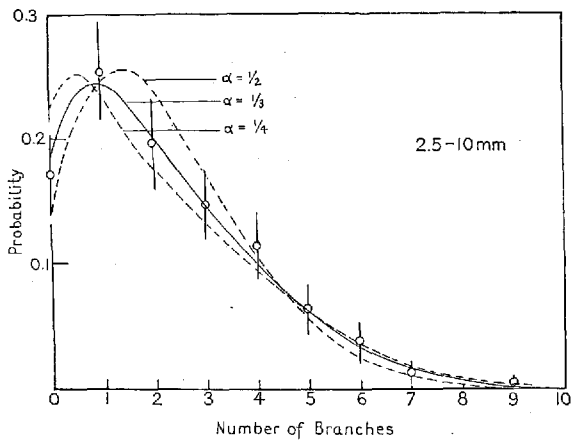

Fig. 4. Distribution of number of branches per track in region 2.5 to 10 mm from end of range.

curve corresponding to $\alpha = 1$ is very small and α is certainly not less than $\frac{1}{2}$, it will be seen that the points in Fig. 4 are much better represented by $\alpha = \frac{1}{3}$ than by $\alpha = \frac{1}{2}$.

From the branch distribution in the interval 2.5 to 10 mm from the end of the range, the presence of two groups of tracks is thus clearly evident, and it is possible without ambiguity to attribute the group with the greater average branch number to the heavy fission fragment. In fact, the average number of branches with lengths between given limits in an interval Δx of the range is given by (cf. ref. 9)

$$\text{(I)} \qquad \omega = 2\pi N \Delta x \frac{(Zze^2)^2}{mV^2}\left[\frac{1}{E_1} - \frac{1}{E_2}\right]$$

where Ze is the nuclear charge of the fragment and ze and m are the charge and mass of the gas nuclei. N is the number of atoms per cubic centimeter, and V is the velocity of the fragment. E_1 and E_2 are the kinetic energies of the branch particles corresponding to the length limits on their tracks. This formula holds in a region where both energy limits represent values which can actually be attained by the struck nuclei, consistent with the requirements of conservation of energy and momentum. We observe that in this case, which corresponds to the experimental conditions except at the extreme end of the range, the number of branches is proportional to $\frac{Z^2}{V^2}$. Assuming that the charges of the nuclear fragments are roughly proportional to their masses, we find that, in the interval from 2.5 to 10 mm, the ratio of the velocity of the heavy particle to that of the light should be either $\frac{V_1}{V_2} = 1.5\sqrt{\alpha} = 0.9$ or $\frac{V_1}{V_2} = \frac{1.5}{\sqrt{\alpha}} = 2.5$. Now, since the heavy particle has an initial velocity which is only $^2/_3$ that of the light particle, it would seem completely excluded that its velocity could exceed the other near the middle of the range by so large a factor as 2.5. Thus, it is clear that the velocity ratio must be given by the first relation above rather than by the second. We conclude thus that, in the range from 2.5 to 10 mm, the velocity of the heavy particle is on the average about 10 % lower than that of the light particle. As regards the interval 0 to 2.5 mm, we have, taking α about $^2/_3$, similarly the choice between $\frac{V_1}{V_2} = 1.2$ or 1.8, and here it is equally clear from the necessary similarity of the two range-velocity curves that

the lower value must be chosen. As pointed out in the note cited above, these deductions from the statistics of the branch distribution are consistent with the theoretical arguments regarding the general character of the stopping phenomenon and with the evidence of the two ranges from the paired fragment tracks.

6. Velocity-Range Curve from the Distribution of Branches.

As indicated in the previous section, the study of the distribution of branches along the tracks of fission fragments offers very direct information regarding the general course of the velocity-range relation. Since, from formula (I) the average velocity of the particle within a given interval of range is strictly proportional to the inverse square root of the number of branches in the interval having lengths within given limits, we can indeed, simply by counting the branches in various sections of the range, obtain the whole curve, at least in relative measure. As a compromise between volume of material and positiveness of identification, branches with lengths in the chamber between 3 and 8 mm inclusive were chosen for this statistics. Since branches of less than 2 mm length are not easily distinguishable close to the end of the range, we have taken 3 mm as a lower limit to exclude the possibility that particular parts of the range would be favoured. In order to test to what extent the upper limit of 8 mm satisfies the condition that all branches in the interval be possible, the average length of the branches between 3 and 8 mm long was determined as a function of the residual range of the fragment tracks. It was found that an approximately constant value of 5 mm obtained over the whole range to within about 1.5 mm (air)

from the end, so the condition may safely be considered to be fulfilled for all residual ranges larger than this value.

The result of the count of 800 branches from 3 to 8 mm in length for the 300 tracks in argon is given in the curve of Fig. 5, where the number of branches per cm of range is given as a function of the residual range, with the probable

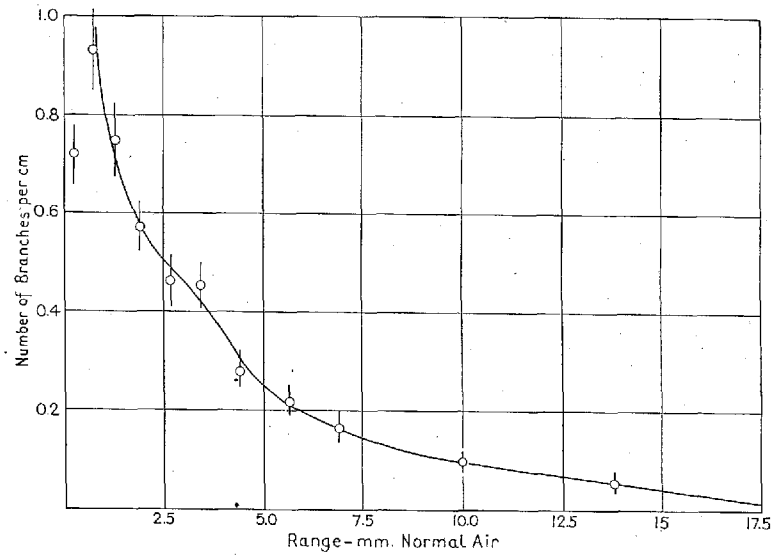

Fig. 5. Distribution of number of branches per cm of track along range.

errors indicated by the vertical lines. The values plotted are compounded from several sets corresponding to various pressures in the cloud chamber. Apart from the first point which is lowered because the velocity of the fragment is too low to give branches of the required length so close to the end of the range, the points lie reasonably well on a smooth curve which falls rapidly for increasing residual range. The evident minimum in the slope of this curve in the region between 2 and 6 mm indicates clearly a flattening off in this region of the velocity-range curve.

To obtain from these data as much information as possible about the range-velocity relation we must, however, in conformity with the conclusions of the preceding section, take the existence of the two groups of fragments into account. In the first place we must remember that the velocities derived by means of (I) from the branch numbers represent a weighted mean of the velocities in the two groups, favouring the heavier particle. Thus, in the portion of the range from 2.5 to 10 mm, where α is about $^1/_3$, three quarters of all the branches come from the heavy particle alone; near the end of the range, where α is probably about $^2/_3$, only about three fifths come from this particle. Since, according to the deduction of the last section, the average ratio between the velocities of the fragments is 0.9 and 1.2 in the two intervals, respectively, one is led to two curves like those indicated in Fig. 6[1]. The circles with the vertical lines in the figure represent the mean values and probable errors of the relative velocities deduced from the branch statistics, the scale being chosen so as to fit as well as possible the absolute measurements of the velocities from individual large branches at the end part of the range, as discussed in the next section. Further, the curves are drawn through the points representing the initial velocities and the mean values for the total range for the two groups derived in section 4.

In an attempt to derive absolute values of the velocities from formula (I), it must be borne in mind that the gas of the chamber is a mixture of argon and saturated alcohol and water vapors. In fact, with an argon pressure of 6 cm

[1] These curves are of quite the same character as those published in the previous note (8). They differ, however, slightly due to corrections which have been made to the ranges and the taking account of new material derived from direct velocity measurements.

as used in this work, the gas contains as many oxygen and twice as many hydrogen atoms as argon atoms. Using the range velocity relation for these particles given by Blackett and Lees (11), we find that only about $^1/_4$ of the branches should be due to argon nuclei, $^1/_4$ to oxygen and $^1/_2$ to hydrogen. The total energy dissipated in each of these

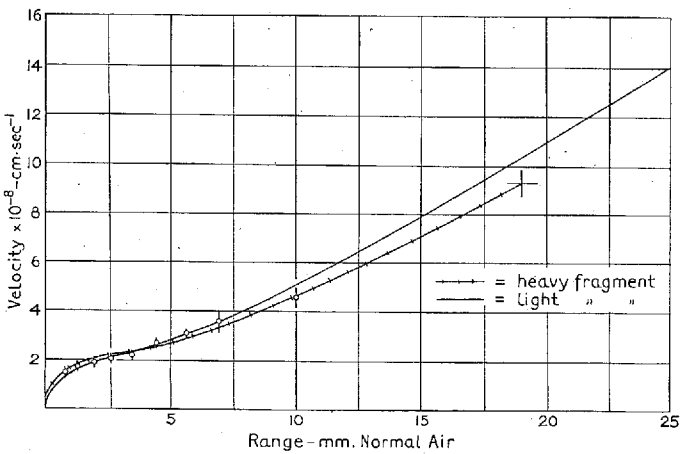

Fig. 6. Velocity-range-curves derived from statistics of branch distribution.

branches is, however, not more than one-half as great for oxygen as for argon and about one-sixth for hydrogen. It is therefore difficult to be sure to what extent the branches due to the lighter particles are included in the count, and in particular, it is probable that practically no hydrogen branches were counted under the experimental conditions. If we assume that all argon and oxygen branches are counted, we obtain a velocity of 3.0×10^8 cm/sec. at a range of 2.5 mm. If, however, we assume that only argon branches are counted, we get 2.0×10^8 cm/sec. at this point. Since the most reasonable run of the curve lies close to the latter value, it seems most probable that only a few of the

oxygen branches are counted in addition to the argon branches.

7. Velocity-Range Determination from Individual Large Branches.

As already pointed out in the preliminary account of the experimental work, the occasional occurrence in the pictures of branches of several centimeters length offers a possibility of directly determining the velocity of the fission fragments from a knowledge of the range-velocity relation of the nucleus making the branch track. From measurements of the angle which the branch makes with the original direction of the fragment and the angle of deflection of the fragment, one can in principle determine the ratio of the velocity of the branch nucleus to that of the fragment itself as well as the ratio of the masses of the two nuclei. In actual practice, however, the frequent small deflections which are characteristic of the tracks of such heavy particles make the measurements of the angles very uncertain. Since the influence of a given error in angle increases with the inverse square of the cosine, this effect makes branches at over sixty degrees useless for such measurements. For close collisions in which the angles are very small and which would otherwise be expected to yield the best values, the uncertainty of the identification of the branch nucleus introduces large errors in the result, both in the determination of the velocity of the branch particle from its range and the ratio of this velocity to that of the stem particle. The final values for the fission fragment velocities thus obtained may differ in some cases by a factor of two, depending on whether the branch is assumed to be oxygen or argon. In the range of angles between 30° and 50°, however, there exists a

region where the result is not sensitively dependent either on the mass ratio or on the angle itself. Thus, if branches within these angle limits are used, the principal uncertainty lies in the determination of the velocity of the struck nucleus from its range; if the range is not too great, the difference in the velocities of oxygen and argon nuclei for a given range is only 10 to 20 %. Thus, taking direct errors of measure-

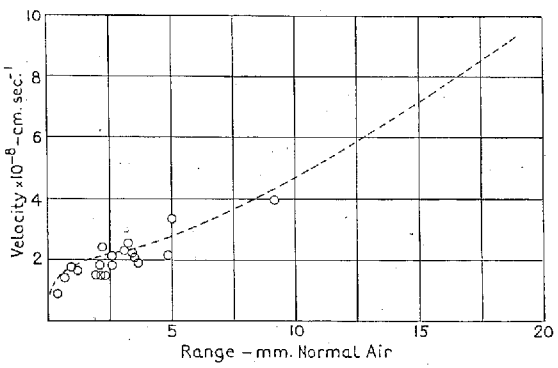

Fig. 7. Velocity-range curve derived from measurements on individual large branches.

ment into account, we might expect a mean error in the determinations of 20 to 30 %. The occurrence of hydrogen branches in the material used would, of course, give an even larger scattering of the values, but it is not considered probable that any others than argon or oxygen are recorded.

Fig. 7 shows the result of twenty-one individual determinations from large branches occurring on tracks in argon. The points represent measurements on branches with angles between 30° and 50°, including only a few exceptional close collisions where it was possible definitely to establish the identity of the branch particle. In the remaining cases, the mass ratio was assumed to be 1:4 and a range-velocity curve for the branch particles lying between those for

oxygen and argon was used. For the range-velocities relation for argon and oxygen, the curves of Blackett and Lees (11) were used, with the values of the velocities increased by five percent (12). The ranges were converted to normal air values by the stopping power coefficients for slow α-particles. As is to be expected from the necessarily rough character of the measurements, the points lie very scattered. Still, as pointed out in the preliminary report, they definitely show that the range-velocity curve is of a type quite different from those found for lighter particles. The dashed curve in the figure represents the range-velocity curve of Fig. 6 corresponding to the heavier fission fragment.

8. Fortuitous Bending.

In order to obtain a quantitative estimate of the effect of small collisions in producing bending of the tracks, measurements of the angle of turning were made at different parts of the range on all the tracks in argon. Tangents to each track in natural size plane projection were drawn at points corresponding to 0.5, 5.5, 10.5, and 15.5 mm (normal air) from the end of the range and their consecutive angles to one another measured with a protractor. The angle between the first and second tangents was called angle "A", between the second and third, angle "B", and that between the third and fourth tangents, angle "C". In all cases where a measurable deflection was made by a branch at a single point, it was subtracted from the result. In general, only sharp angles of more than five degrees could be so eliminated.

Fig. 8 shows the results for the three portions of the range. The points represent the probability derived from the measurements for the occurrence of angles within the intervals indicated by the abscissae. The scales are chosen

roughly proportional to the square roots of the number of measurements in each of the three groups so that the probable errors are comparable in the figure. Through these experimental points are fitted curves of the form $e^{-\frac{x^2}{2\Phi^2}}$. It is quite obvious that the curvature is by far the

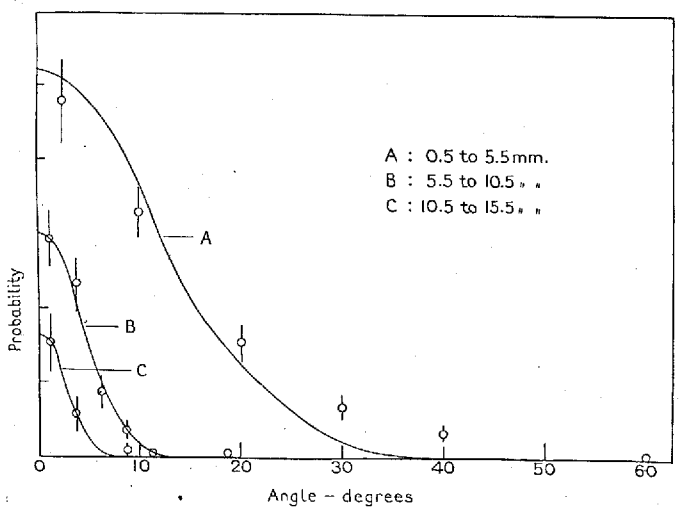

Fig. 8. Bending of tracks in various regions of range.

greatest near the end of the range where nuclear collisions are so frequent. The curvature represented by angle "C" is almost within the error involved in drawing the tangents. For large angle scattering the points lie considerably higher than the Gaussian curve, as is to be expected (9) since such collisions occur on the average less than once in every track.

According to Bohr (5), the mean square deviation of a track should be given approximately by

$$\Phi^2 = \frac{m_2}{m_1}\frac{\Delta T}{T}\left(\frac{\Delta_n T}{\Delta T}\right) \qquad \text{(II)}$$

where m_1 and m_2 are the masses of the fission fragment and the struck particles respectively; $\frac{\Delta T}{T}$ is the fractional energy loss in the interval considered and the term in parentheses represents the part of the stopping which is due to nuclear collisions. Assuming, as a first approximation, that all the deflections arise from collisions with argon nuclei, we have

$$\frac{\Delta_n T}{\Delta T} = \frac{1}{3}, \frac{1}{16}, \frac{1}{40}$$

for the three portions of the range, remembering that the mean square curvature measured on a plane projection should be multiplied by two to obtain the value representing the deflection in space. From these figures, it is quite clear that nuclear collisions which are responsible for the ultimate stopping are already of considerable importance in the last quarter of the range. Although no measurements have been made on the tracks in hydrogen, inspection of the pictures shows that the curvature is very much less in this case, as would be expected from formula (II).

9. Rate of Energy Loss along Range.

The details of the stopping effects are particularly clearly illustrated from the variation of the energy loss per unit length along the range, which can be simply deduced from the range velocity curve. The results obtained by differentiating the square of the curve of Fig. 6 for the heavier fission fragment is given in Fig. 9, where the rate of energy loss for an alpha particle along the same part of the range is also given (12). While the latter curve exhibits a maximum near the end of the range, the curve for the fission fragments

shows a definite minimum in about the same part of the range. This difference between the two curves illustrates clearly the very different character of the stopping mechanisms in this region. For the alpha particle curve the maximum represents the onset of the influence of electronic capture in reducing the charge effective in electronic inter-

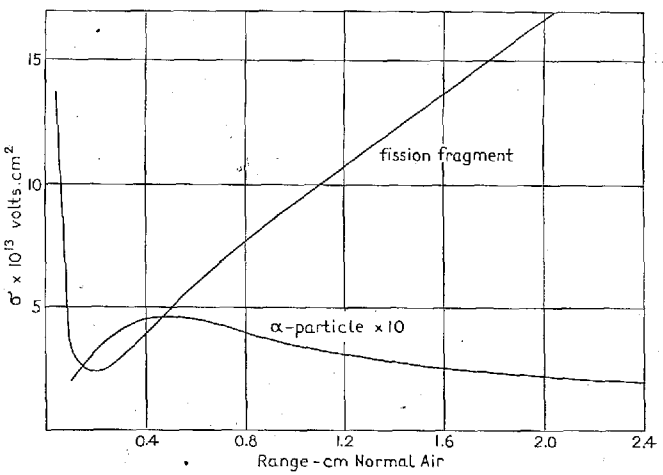

Fig. 9. Rate of energy loss along range for fission fragments, with corresponding function for alpha-particles plotted for comparison.

actions which here are practically determining for the whole stopping effect. For the fission fragments, however, the initial decrease in the rate of energy loss is due to the continual increase of the number of captured electrons along the whole range and the rapid rise at the end reflects the increasing preponderance of the stopping effect of nuclear collisions for the lowest velocities. It is interesting to notice that the striking differences between the two curves can in some way be considered as due to a difference in scale of the representation of corresponding effects. In fact, the range-

velocity curve obtained here for fission fragments might be taken as a rough indication of the behaviour of lighter particles very close to the end of their range. Still, as it appears from formula (II), we will for such light particles in air or heavier gases, have an extraordinary degree of scattering near the extreme end of the range where the stopping due to nuclear collisions becomes essential. These points are more closely discussed in the theoretical paper (9) of Professor Bohr to which repeated reference has been made in the foregoing.

10. Summary.

Certain general features of the penetration of uranium fission fragments through matter as revealed by the study of several hundred cloud chamber photographs in various gases are discussed. In particular, it is shown that a study of the large number of conspicuous branches gives much information about the problem of the stopping of such heavy particles. It is shown that it is possible by analysis of the branch distribution to divide the tracks into two groups, representing fragments with different charge and mass, and to derive from a count of the branches at various parts of the range separate velocity-range relations for each group. The curves obtained clearly reflect the influence of electron capture all along the range in a steady linear fall over most of the range, and the effect of nuclear collisions in a sharp descent at the end. The curve between these two parts is characterized by a definite flattening off, where the rate of velocity loss is a minimum. By the independent method of measuring angles and lengths of particularly long branches, a velocity-range relation of the same general character is obtained, although the rather large experimental errors do not permit a detailed comparison. In addition, it is shown that a general bending is characteristic of the paths of fission fragments and occurs in connection with the nuclear stopping. A comparison of the rate of energy loss of such fragments with that of alpha particles emphasizes the differences in the stopping mechanisms, indicating a definite minimum in energy loss near the end of the range, in the same region where an alpha particle has a maximum energy loss.

The work has been carried out at the Institute of Theoretical Physics in Copenhagen under the direction of Professor Bohr, for whose active help and continued encouragement the authors are deeply grateful. We are much obliged to Dr. Jacobsen, who pointed out the optical system used for measuring the films and helped us with the necessary adjustments. Our thanks are also due Mr. A. Lundbak, Mr. K. Lindberg-Nielsen, Miss L. Bakander and Miss I. Jensen, whose help in the laboratory work has been of great value.

References.

(1) F. Joliot, Comptes Rendus 9, 647 (1939).
(2) D. R. Corson and R. L. Thornton, Phys. Rev. 55, 509 (1939).
(3) N. Perfilov, C. R. Acad. Sc. URSS XXIII, 896, 1939.
(4) K. J. Brostrøm, J. K. Bøggild and T. Lauritsen, Phys. Rev. (1940).
(5) N. Bohr, Phys. Rev. (1940).
(6) Cf. L. H. Turner, Rev. Mod. Phys. **12**, 1 (1940).
(7) L. Meitner and O. R. Frisch, D. Kgl. Danske Vidensk. Selskab, Math.-fys. Medd. **XVII**, 5 (1939).
(8) N. Bohr, J. K. Bøggild, K. J. Brostrøm and T. Lauritsen, Phys. Rev. (in press).
(9) N. Bohr, D. Kgl. Danske Vidensk. Selskab, Math.-fys. Medd. (in press).
(10) T. Bjerge, K. J. Brostrøm, J. Koch and T. Lauritsen, D. Kgl. Danske Vidensk. Selskab, Math.-fys. Medd. **XVIII**, 1 (1940).
(11) P. M. S. Blackett and D. S. Lees, Proc. Roy. Soc. **134**, 660 (1931).
(12) M. S. Livingston and H. A. Bethe, Rev. Mod. Phys. 9, § 95 (1937).

11. Description of Plates.

Plate I a, b, c.

(0.25 natural size).

Stereoscopic pictures of tracks in hydrogen. Particle originates in uranium coating on copper strip (white crescent) near wall of chamber. Fine parallel lines are wires fastened to the underside of glass cover to provide conducting surface for sweep field. ($H_2 + \frac{1}{6} C_2H_6O + \frac{2}{3} H_2O$, total pressure 13 cm) (photographed with single mirror system: mirror image reversed in reproduction).

Plate II a.

(0.4 natural size).

Track in argon originating in lower left hand corner of picture; shows fortuitous bending and characteristic tuft at end as well as several discontinuities caused by reduction of local supersaturation by earlier proton or α-particle tracks. ($A + 20\,\% O_2 + \frac{1}{2} C_2H_6O + \frac{1}{2} H_2O$, total pressure 6.5 cm).

Plate II b.

(0.4 natural size).

Track in low pressure hydrogen with many fine proton branches in addition to one branch resulting from a collision with an oxygen nucleus. ($H_2 + H_2O$, total pressure 14 cm).

Plate III a.

(0.4 natural size).

Direct picture and mirror picture of close collision of fission fragment with argon nucleus. Argon branch proceeds nearly three times farther than fission fragment and shows considerable bending. Fission fragment is clearly recognizable from the large number of branches. ($A + 20\,\% O_2 + \frac{1}{2} C_2H_6O + \frac{1}{2} H_2O$, total pressure 6.5 cm).

Plate III b.

(0.4 natural size).

Close collision with argon nucleus showing abrupt change of ionization of fragment track due to sudden decrease of velocity. Argon branch shows secondary branching. ($A + C_3H_8O$, total pressure 7 cm).

Plate IV a.

(0.7 natural size).

Close collision with argon nucleus: end of main track indicated by arrow 1. At arrow 2, branch particle collides with another argon nucleus separating from it at an angle of 90°. ($A + H_2O$, total pressure 6.5 cm).

Plate IV b.

(0.4 natural size).

Track in argon with close collision at end of range. ($A + 20\,\%$ $O_2 + \frac{1}{2}\,C_2H_6O + \frac{1}{2}\,H_2O$, total pressure 6.5 cm).

Plate V a.

(0.4 natural size).

Double fragment track originating in left hand side of 0.3 mg/cm² aluminum foil held on support in center of chamber. ($A + \frac{1}{2}\,C_2H_6O + \frac{1}{2}\,H_2O$, total pressure 27 cm).

Plate V b.

(0.4 natural size).

Double fragment track originating in right hand side of 1.2 mg/cm² mica foil held on support in center of chamber. ($A + H_2O$, total pressure 20 cm).

Plate VI a.

(0.4 natural size).

Track in argon with collision with oxygen nucleus resulting in branch suitable for velocity determination. ($A + C_3H_8O$, total pressure 7 cm).

Plate VI b.

(0.7 natural size).

Particularly intense track, showing several branches, all more intense than proton and α-ray tracks appearing as background. ($A + \frac{1}{2}\,C_2H_6O + \frac{1}{2}\,H_2O$, total pressure 10 cm).

Indleveret til Selskabet den 7. September 1940.
Færdig fra Trykkeriet den 7. November 1940.

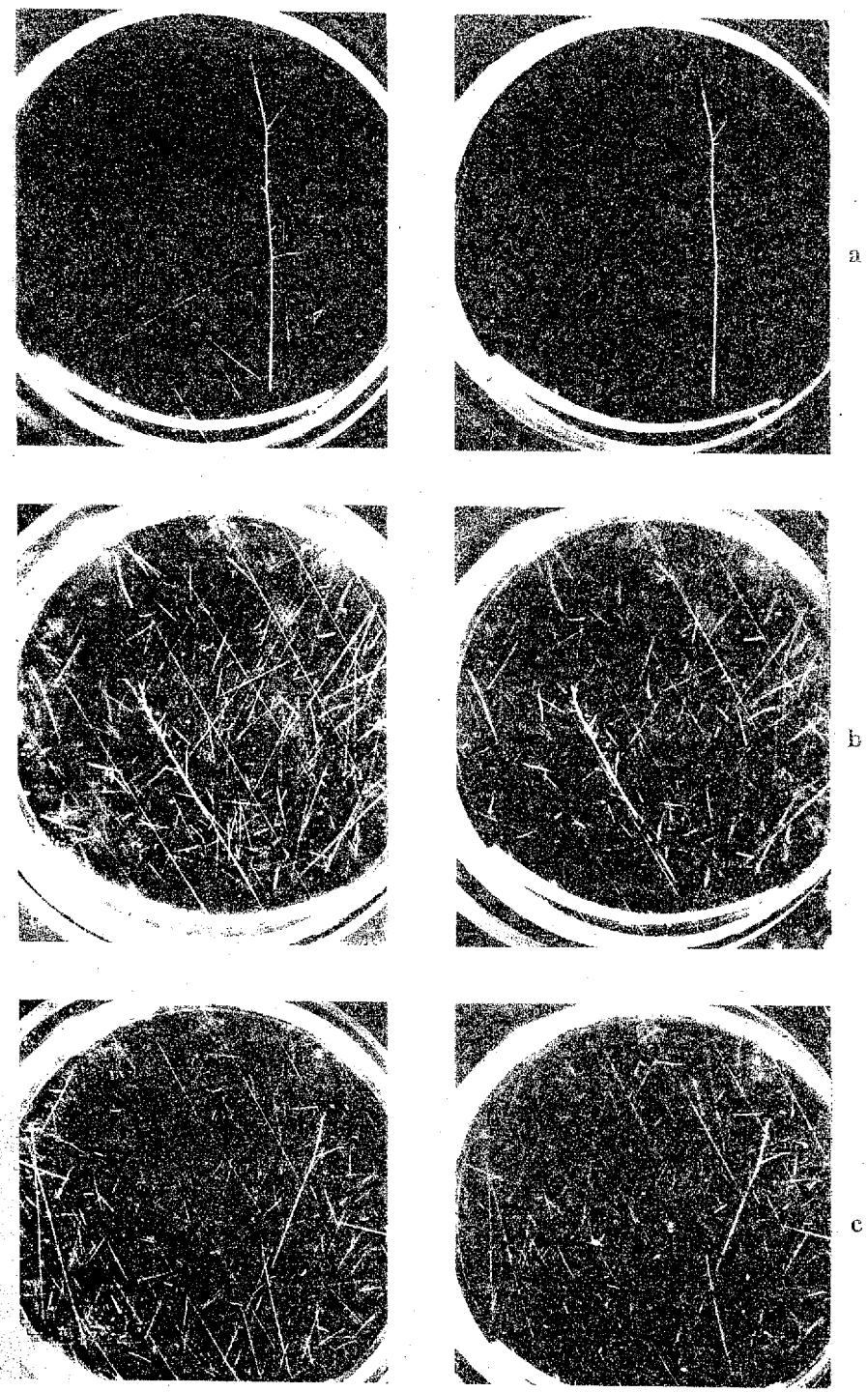

Plate IV a.

(0.7 natural size).

Close collision with argon nucleus: end of main track indicated by arrow 1. At arrow 2, branch particle collides with another argon nucleus separating from it at an angle of 90°. ($A + H_2O$, total pressure 6.5 cm).

Plate IV b.

(0.4 natural size).

Track in argon with close collision at end of range. ($A + 20\ \%$ $O_2 + \frac{1}{2} C_2H_6O + \frac{1}{2} H_2O$, total pressure 6.5 cm).

Plate V a.

(0.4 natural size).

Double fragment track originating in left hand side of 0.3 mg/cm² aluminum foil held on support in center of chamber. ($A + \frac{1}{2} C_2H_6O + \frac{1}{2} H_2O$, total pressure 27 cm).

Plate V b.

(0.4 natural size).

Double fragment track originating in right hand side of 1.2 mg/cm² mica foil held on support in center of chamber. ($A + H_2O$, total pressure 26 cm).

Plate VI a.

(0.4 natural size).

Track in argon with collision with oxygen nucleus resulting in branch suitable for velocity determination. ($A + C_3H_8O$, total pressure 7 cm).

Plate VI b.

(0.7 natural size).

Particularly intense track, showing several branches, all more intense than proton and α-ray tracks appearing as background. ($A + \frac{1}{2} C_2H_6O + \frac{1}{2} H_2O$, total pressure 10 cm).

Indleveret til Selskabet den 7. September 1940.
Færdig fra Trykkeriet den 7. November 1940.

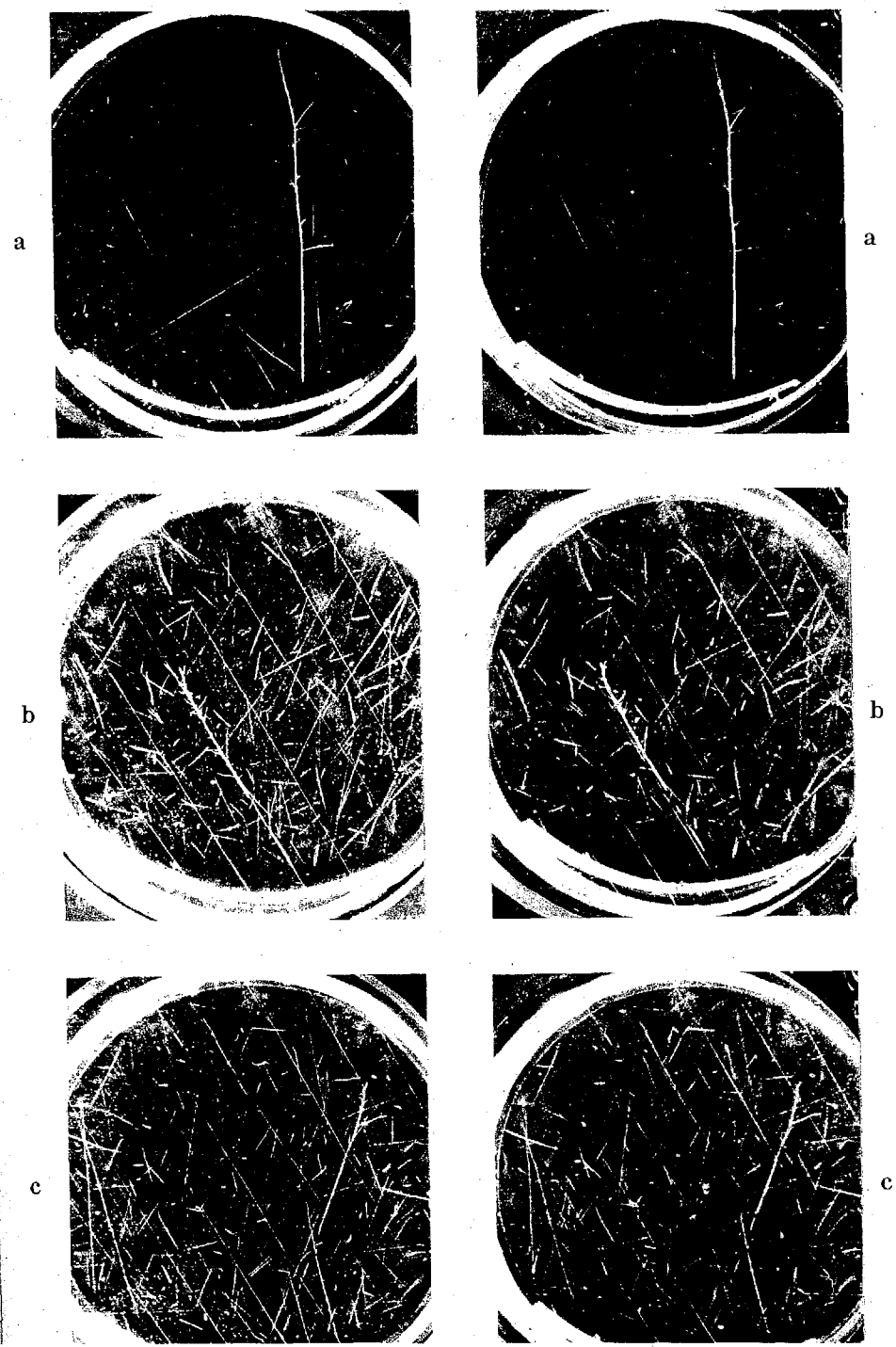

a

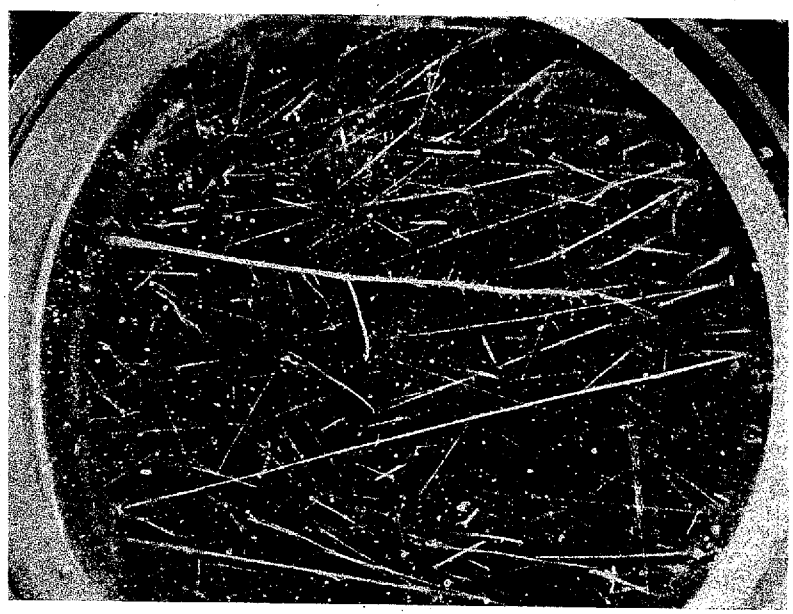

b

a

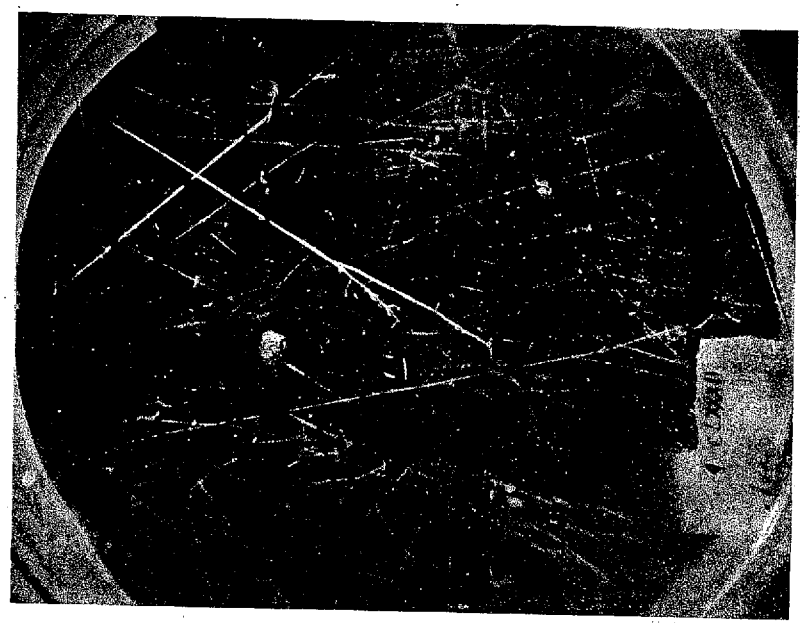

b

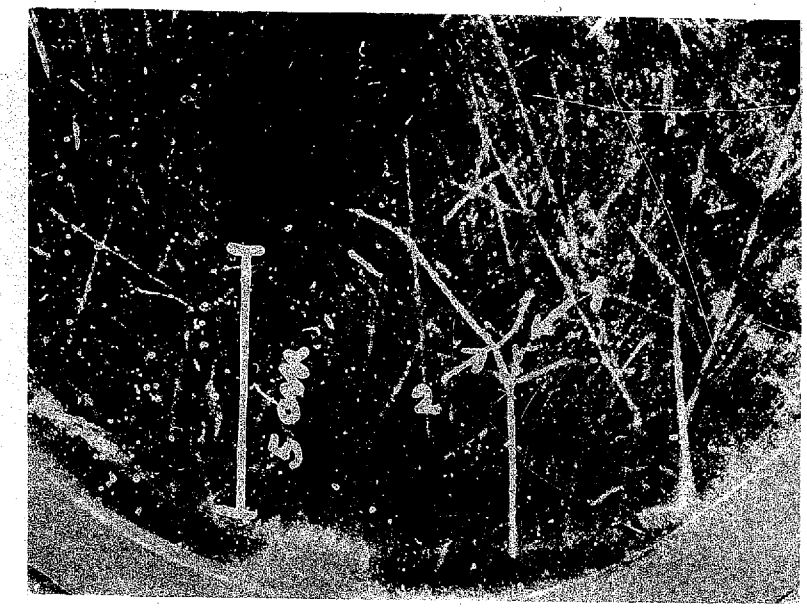

a

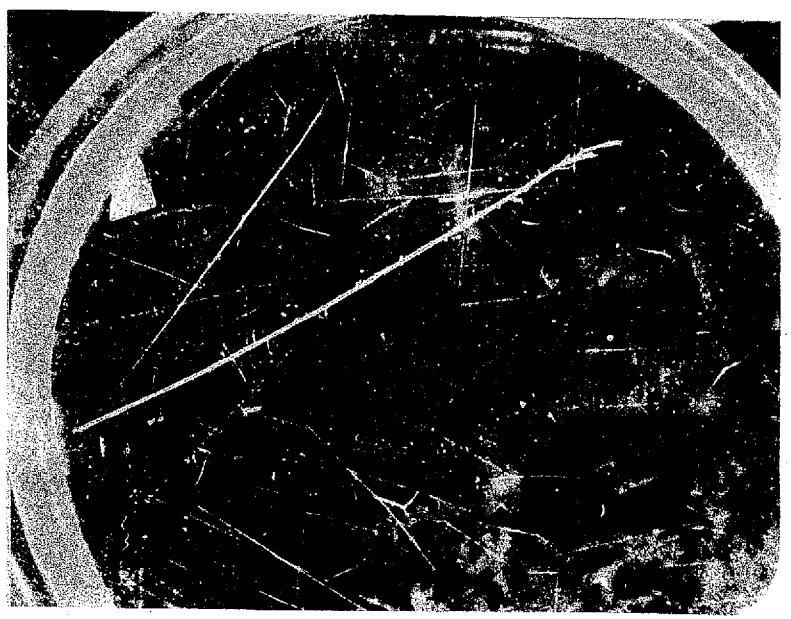

b

a

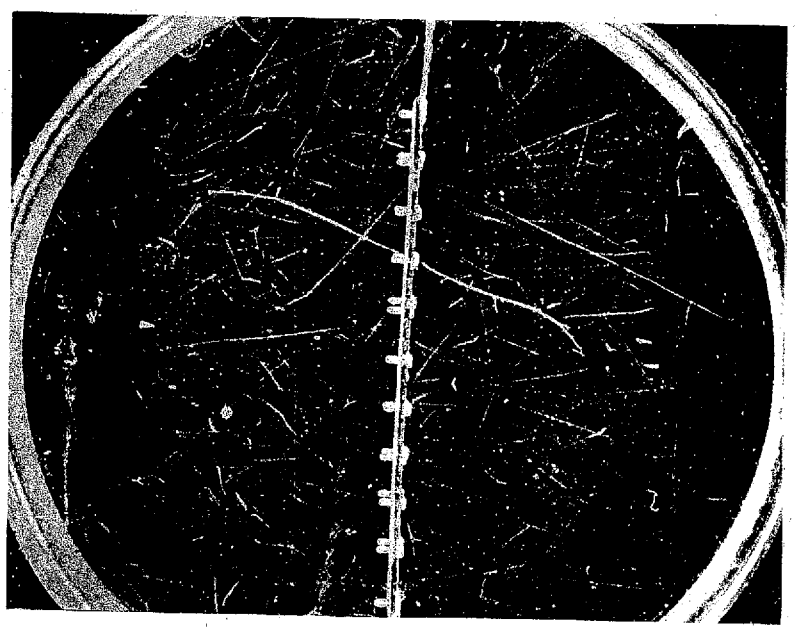

b

a

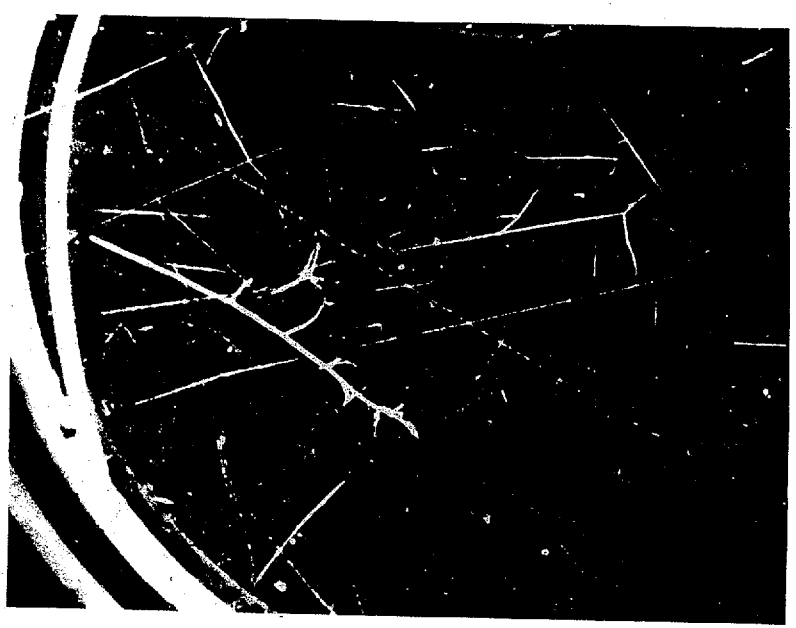

b